HBRP
PUBLICATION

Journal of Emerging Trends in Electrical Engineering
Volume 3 Issue 1

Particle Swarm Optimized Phase Shifted DVR (PSDVR) for High Voltage Ride through in DFIG

***Sheena Latif*[1] *, Savier J. S.*[2]**
[1]**Dept. of EEE, College of Engineering, Trivandrum, Kerala, India*
[2]*Dept. of EEE, Govt. Engineering College, Palakkad, Kerala, India*
Corresponding Author
E-Mail Id: sheenalatif@gmail.com

ABSTRACT

Doubly fed Induction Generators have gained attention among wind power manufacturers across the globe, owing to its benefits of partially rated converters and stable performance during variable wind speed conditions. DFIGs are very sensitive to grid voltage sag or swell conditions. The low voltage ride through of DFIG during voltage sag has been a sensitive area of research for the past decade. A more serious issue now gaining interest among researchers world-wide is high voltage ride through (HVRT) of DFIG based wind farms. A sudden disconnection of connected inductive load or transformers or improper switching can lead to the voltage swell condition of grid connected DFIG. The rise in voltage has its effects on the stator flux and current of DFIG and its consequences on the magnetically coupled rotor and its converters. HVRT is a relatively new area of research and the various possibilities of HVRT technologies are still being investigated. This paper proposes a promising solution for HVRT of DFIG using Phase Shifted Dynamic Voltage Restorer (PSDVR) with governing equations and design considerations. The simulation is carried out in MATLAB/SIMULINK and the obtained results justify the analogy of Phase Shifted DVR for HVRT in DFIG. The DVR controllers are optimized using Particle Swarm Optimization (PSO) algorithmic MATLAB.

Keywords: *Doubly fed induction generator, phase shifted DVR, voltage swell, high voltage ride through*

INTRODUCTION

The wind power generation and distribution has taken a tremendous boom in the renewable energy industry through the last few decades. The influence of wind power penetration in the distribution side of power system is expanding sharply. Among the various wind power generators the variables peed wound rotor Doubly Fed Induction Generator (DFIG) is the most popular one. The power rating of converters used in the rotor side of DFIG is slip times the stator power. More over the generator produces power from stator as well as rotor during super synchronous mode of operation. DFIG has excellent steady state operation characteristics during variable speed but also are extremely sensitive to grid disturbances. The stator is directly connected to grid while the rotor interacts with the grid through converters. Rotor over voltage can harm the rotor side converters (RSC) during voltage sag or swell condition.

The dynamic behavior of DFIG during balanced and unbalanced voltage dip is studied in literature [1-3]. Suggested solutions for Low Voltage Ride Through (LVRT) of DFIG includes series dynamic braking resistors, modified rotor current control strategies, crow bar resistors and FACTS devices[4-7]. Dynamic voltage restorer has been suggested as a solution to voltage sag of DFIG by voltage restoration in literature[8,9]. LVRT technologies have

made their position in the wind farms as grid code requirements regarding LVRT are made mandatory by all countries.

The wind market is looking towards a more serious issue compared to LVRT which is high voltage ride through (HVRT) in DFIG. Very few literatures have been effective enough to trace the real consequences of HVRT in DFIG[10-12]. HVRT requirements are gradually expected to be made mandatory by all countries who supply wind power. The dynamic behavior of DFIG during a voltage swell condition is studied in detail in this paper. The possibility of DVR as a voltage restorer during voltage swell of grid connected DFIG is exploited in the proposed paper. The PID controllers used for DVR is optimized using Particle Swarm Optimization (PSO) algorithm [13,14] and control is carried out in dq reference frame. No additional hardware are required for converting the DVR to Phase Shifted DVR (PSDVR) thus making the proposed control strategy of DVR cost effective for wind farms already equipped with DVR schemes.

The proposed paper is broadly classified into the following sections. Section II deals with dynamic behavior of DFIG during voltage swell and its governing equations. Section III comprises of PSDVR and its control algorithm in synchronous reference frame. The PSO optimized PID values are utilized in the PSDVR for reducing the rise in voltage. The design considerations of PSDVR for HVRT are also discussed in this section. Section IV discusses the results that justify the effectiveness of the proposed PSDVR in tackling HVRT in DFIG and Section V concludes the proposed work.

DFIG OPERATION

DFIG during Normal Operation

The equivalent circuit of DFIG is as shown in Figure 1. The behavior of DFIG during normal operation and during swell are analyzed using this equivalent circuit. The basic equations of DFIG referred to stator variables are given from (1)-(4) as per [1]. The meanings of symbols are as follows:$\vec{v}_s$, $\vec{v}_r$ are stator and rotor voltage vectors $\vec{\imath}_s$,$\vec{\imath}_r$ the stator and rotor current vectors $\vec{\psi}_s$, $\vec{\psi}_r$ the stator and rotor flux vectors respectively. L_m is the mutual inductance between stator and rotor while L_s, $L_r$the self-inductances of stator and rotor windings including the leakage inductances respectively.

$$\vec{v}_s = R_s\vec{\imath}_s + \frac{d\vec{\psi}_s}{dt} \quad (1)$$

$$\vec{v}_r = R_r\vec{\imath}_r + \frac{d\vec{\psi}_r}{dt} - j\omega\vec{\psi}_r \quad (2)$$

$$\vec{\psi}_s = L_s\vec{\imath}_s + L_m\vec{\imath}_r \quad (3)$$

$$\vec{\psi}_r = L_r\vec{\imath}_r + L_m\vec{\imath}_s \quad (4)$$

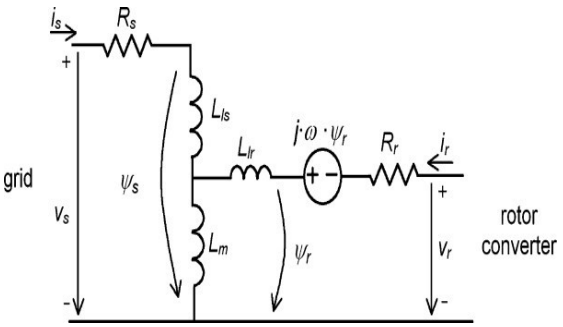

Fig.1: *DFIG Equivalent Circuit Referred to Stator*

The rotor voltage can be calculated from (2) and is obtained as in (5) with RSC connected to the rotor. The first term represents the open circuit rotor voltage when rotor is open circuited and depends only on stator flux. The second term is related to rotor current and also the transient inductance term σL_r, where σ is given by (6). The stator flux vector rotates at synchronous speed with steady state magnitude Ψ_{sf}as shown in (7) and stat or voltage vector rotates with constant magnitude of V_s with synchronous speed as given in (8) during normal operation of DFIG.

$$\vec{v}_r = \frac{L_m}{L_S}\left(\frac{d}{dt} - j\omega\right)\vec{\psi}_S + \vec{i}_r\left(R_r + \sigma L_r\left(\frac{d}{dt} - j\omega\right)\right) \quad (5)$$

$$\sigma = 1 - \frac{L_m^2}{L_S L_r} \quad (6)$$

$$\vec{\psi_S} = \Psi_{sf} e^{j\omega_S t} \quad (7)$$

$$\vec{v_S} = V_s e^{j\omega_S t} \quad (8)$$

DFIG during Voltage Swell

Let the voltage magnitude at time $t < t_0$ be V_1. At time $t = t_0$, a voltage swell appears in the grid. For $t \geq t_0$ the magnitude of stator voltage changes to V_2 and can be expressed in terms of V_1 as in (9), where p is the voltage swell ratio.

$$\vec{v}_S = \begin{Bmatrix} V_1 e^{j\omega_S t} & \text{for } t < t_0 \\ (1+p)V_1 e^{j\omega_S t} & \text{for } t \geq t_0 \end{Bmatrix} \quad (9)$$

The stator flux consists of sum of two components: the steady state flux and natural flux. The steady state flux $\vec{\psi}_{sf}$ before and after voltage swell is given by (10). The natural flux $\vec{\psi}_{sn}$ ensures the continuity in stator flux when the flux magnitude changes proportionally with stator voltage. This component of flux appears only during transient condition of sag or swells and is given as in (11). As evident from (11), the transient flux dies out with stator time constant τ_S, and has an exponentially diminishing negative dc value and is proportional to the ratio of swell. If the height of swell is larger initial magnitude of natural flux will increase proportionally. The magnitude of steady state flux after swell is proportional to the stator voltage after swell[9].

$$\vec{\psi}_{sf} = \begin{Bmatrix} \frac{V_1}{j\omega_S} e^{j\omega_S t} & \text{for } t < t_0 \\ \frac{(1+p)V_1}{j\omega_S} e^{j\omega_S t} & \text{for } t \geq t_0 \end{Bmatrix} \quad (10)$$

$$\vec{\psi}_{sn} = \frac{-pV_1}{j\omega_S} e^{-(t-t_0)/\tau_S} e^{j\omega_S t_0} \quad (11)$$

The stator voltage swell has influence on rotor voltage of DFIG. The rotor voltage also comprises of steady state and natural components and is the effective sum of these two. The rotor voltage natural component vector $\vec{v}_{rn}$ is given by (12). It is evident from (12) that $\vec{v}_{rn}$ is proportional to $(1-s)$ and height of rise, where is the slip of DFIG. The operating range of slip of DFIG is too small usually $\pm 25\%$ and hence the value of natural component will be higher. If the height of swell is small the value of $\vec{v}_{rn}$ will not cause serious effects on RSC. If the swell height is considerably larger it can damage the RSC of DFIG. The steady state rotor voltage after swell $\vec{v}_{rf2}$ is proportional to DFIG stator voltage magnitude after swell as well as slip as given in (13). The effective rotor voltage with RSC connected to rotor will be the sum of steady state and natural components as shown in (14).

$$\vec{v}_{rn} = \frac{L_m}{L_S}(pV_1)(1-s)e^{-\frac{t}{\tau_S}} \quad (12)$$

$$\vec{v}_{rf2} = \frac{L_m}{L_S}(1+p)V_1 s e^{j\omega_S t} \quad (13)$$

$$\vec{v}_r = \vec{v}_{rn} + \vec{v}_{rf2} + \vec{i}_r\left(R_r + \sigma L_r\left(\frac{d}{dt} - j\omega\right)\right) \quad (14)$$

PROPOSED PHASE SHIFTED DYNAMIC VOLTAGE RESTORER FOR VOLTAGES WELL COMPENSATION

Dynamic Voltage Restorer is a proven topology for voltage restoration in distribution systems during voltage sag conditions. DVR consists of three phase inverter coupled to grid using series transformer. The inverter output is filtered and fed in series with the grid in magnitude to the voltage to be injected with the required phase angle shift. The basic structure of DVR with DFIG is as shown in Figure 2.

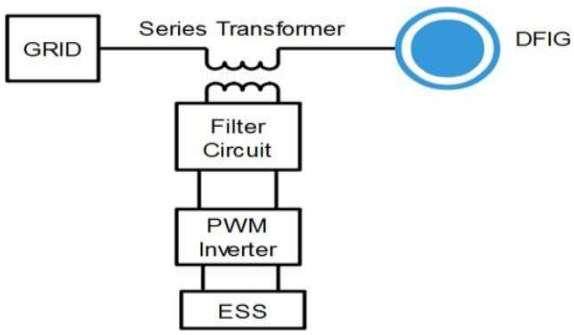

Fig. 2: *DVR in Series with Grid Connected DFIG.*

DVR Control Strategy during Voltage Sag

In the control strategy of DVR for voltage sag compensation, the stator voltages of DFIG in all the three phases are monitored and compared with rated values in synchronous reference frame. The error is minimized using PID controllers whose outputs are converted to three phase voltage values and fed to pulse generator. The pulses generated will drive the inverter of DVR and will inject the depth of sag voltage to restore the stator voltage. Usually the voltage injected is in phase with sag voltage in the absence of phase angle jumps and in phase with pre-sag voltage in case of any phase angle jumps.

Proposed PSDVR Control Strategy with PSO Optimization during Voltage Swell

In the case of HVRT, voltage to be injected by PSDVR should be out of phase with the stator voltage and in magnitude with the height of swell. This is made possible by the control strategy of the proposed PSDVR. The measured stator voltage with swell is phase shifted by 180°.

This three phase voltage is Park's transformed to direct and quadrature axis values and fed to error calculator with the referenced q voltage values. The error will be obtained as pV_1 and corresponding two axis values are generated by the PID controller. This is inverse Park's transformed to three phase voltages and fed as modulating signal to pulse generator. This activates the inverter of PSDVR to inject voltage with a phase shift of 180in series with the grid. This method helps in reducing voltage swell during HVRT of DFIG. The control strategy of PSDVR is shown in Figure 3.

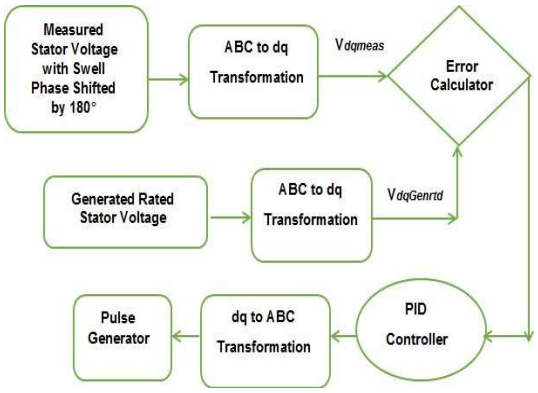

Fig. 3: *PSDVR Control Block Diagram.*

The transfer function of three phase inverter is obtained to be where K_{IN} is the gain of the inverter obtained from the given dc input voltage and T_{IN} is the time delay equal to carrier switching cycle time of the inverter. The transfer function of filter $G_{INV} = \frac{K_{IN}}{1+ST_{IN}}$, Where the filter impedance

$$G_{FILTER} = \frac{Z_L}{s^2LC+s(L+RCZ_f)+R+Z_f}$$

The transfer functions of the PID controller $G_{PID} = K_P + \frac{K_I}{s} + K_D.s$. The total transfer function of the PSDVR with PID controller in open loop is obtained as G_F given by (15). The block diagram representation of transfer function of PSDVR is as shown in Figure 4.

$$G_F = G_{PID} * G_{INV} * G_{FILTER} \quad (15)$$

Particle Swarm Optimization is a stochastic, population-based evolutionary computer algorithm for problem solving. Particles update their velocities based on the combined effect of current motion, particle own memory and swarm influence. This algorithm is used to optimize the PID controller values in d and q axis. The velocity update equation of PSO algorithm is given in (16).

$$v_{k+1}^i = wv_k^i + c_1 rand\frac{(p^i - x_k^i)}{\Delta t} + c_2 rand\left(\frac{p_k^g - x_k^i}{\Delta t}\right) \quad (16)$$

The new velocity of a swarm of birds is v_{k+1}^i based on the current motion wv_k^i, particle memory influence $\frac{(p^i - x_k^i)}{\Delta t}$ and swarm influence $\left(\frac{p_k^g - x_k^i}{\Delta t}\right)$ respectively. In (16) is the bird inertia factor with a range of 0.4 to1.4, C_1 the self-confidence of the range 1.5 to 2 and C_2 the self-confidence for global best position respectively. The algorithm code is run in MATLAB and the optimal values of PID controllers are obtained as $K_P = 0.622$, $K_I = 2.89$ and $K_D = 1.5$ for d-axis and $K_P = 0.203$, $K_I = 3.85$ for q-axis respectively.

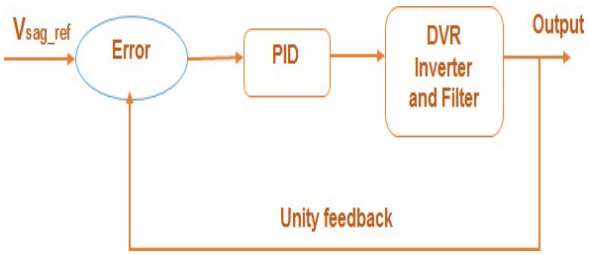

Fig. 4: *Block Diagram Representation of PID controlled PSDVR.*

Design Considerations of PSDVR

DVR is designed for *m*% compensation of stator voltage usually within the range of ±25%. The power rating of PSDVR designed for HVRT support of DFIG with capacity P_{DFIG} should be as given in (17).

$$P_{PSDVR} = \frac{P_{DFIG}(1-(1+m\%)^2)}{3} \quad (17)$$

The voltage to be injected across the capacitor of the filter is V_C and with *m*% compensation is given by (18) where *k* is the transformer ratio of series injection transformer.

$$V_C = \frac{mV_S}{100k} \quad (18)$$

The equivalent resistance R_L offered by PSDVR on the dc source of inverter V_{DC} is given in (19). The filter design is based on the resonant frequency f_c of LC filter as in (20) respectively.

$$R_L = \frac{V_{DC}^2}{P_{PSDVR}} \quad (19)$$

$$f_c = \frac{1}{2\pi\sqrt{LC}} \quad (20)$$

RESULTS AND DISCUSSIONS

The simulation is carried out for a grid connected DFIG of 1.5 MW and stator voltage 575V. The 22kV grid is connected to DFIG using step up transformer 575V/22kV. The DFIG data used for simulation is provided in Appendix.

DFIG with Asymmetrical Voltage Swell

The DFIG behavior during a voltage swell is analyzed for 100ms duration from 0.05 to 0.15s for asymmetric conditions. The stator voltage is allowed to rise upto 1.2p.u. Since the designed PSDVR has a compensation capacity of 20%, the 1.2 p.u of stator voltage can be reduced to1p.u. by the designed PSDVR. The parameters of designed PSDVR are given in Appendix as Table 2.

The stator voltage swell in A and B phases and corresponding stator flux trajectory are shown in Figure 5a) to5b) respectively. The stator voltage and flux follows the governing equations (9) and (10) as evident from the results. The radius of stator flux trajectory increases to the new steady state value during voltage swell as observed from Figure 5b). The C phase continues healthy operation and no PSDVR action is required. The natural flux due to voltage swell dies out very fast as seen from the results. The steady state rotor voltage during swell rises proportional to stator flux and thereby the dc link capacitor voltage of DFIG rotor side converter rises with fluctuations from 1100 V to 1200V as shown in Figure 5c).

By the application of PSDVR the swell in stator voltage is restored to rated value. As the stator voltage is restored to rated value, the flux also gets restored to pres well

condition as seen from Figure 6a). The stator flux remains almost stable with the action of PSDVR and the rotor voltage rise is minimized causing a stabled clink capacitor voltage as shown in Figure 6b) and 6c) respectively. The dc link fluctuation is reduced to within 1120V to 1165V by the PSDVR action. The operation of proposed PSDVDR is found satisfactory in the case of asymmetrical voltages well as depicted by the results.

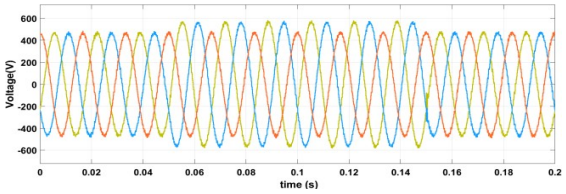

Fig. 5(a): *Stator voltage with 1.2p.u Swell in A and B Phases.*

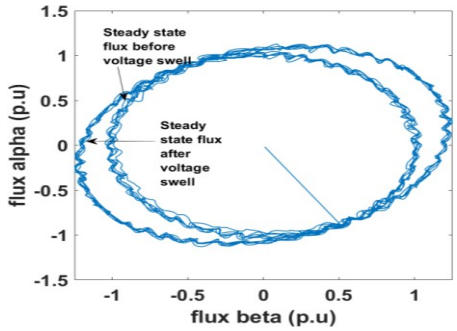

Fig. 5(b): *Stator Flux Trajectory under Asymmetrical Voltage Swells.*

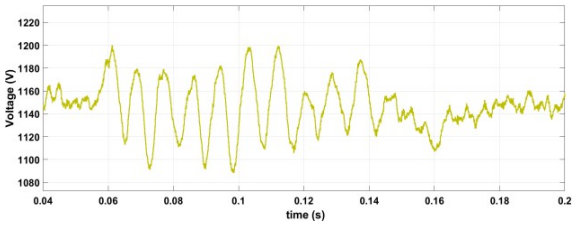

Fig. 5(c): *DC Link Capacitor Voltage during Asymmetrical Voltage Swell.*

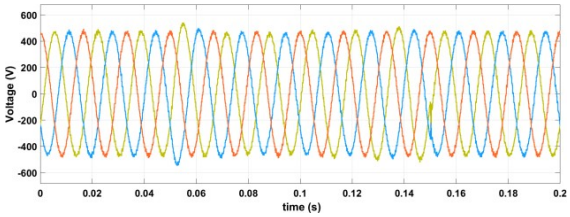

Fig. 6(a): *PSDVR Restored Stator Voltage during Asymmetrical Voltage Swell.*

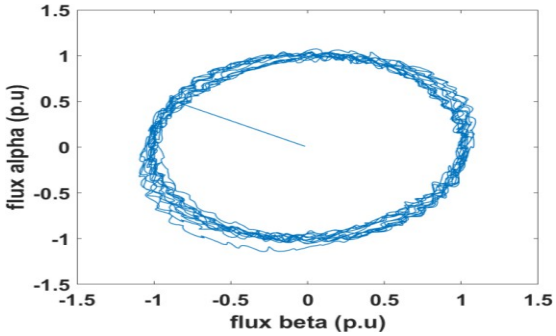

Fig. 6(b): *PSDVR Restored Stator Flux Trajectory during Asymmetrical Voltage Swell.*

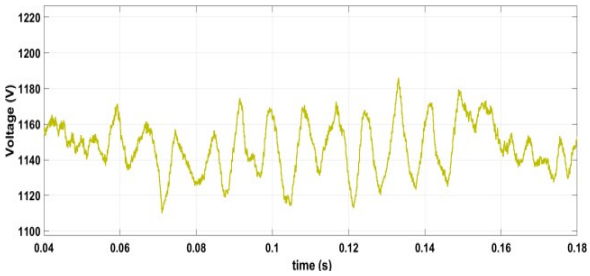

Fig. 6(c): *DC Link Capacitor Voltage after PSDVR Action.*

DFIG with Symmetrical Voltage Swell

A symmetrical voltage swell of 1.2 p.u is applied at stator side of DFIG from 0.05 to 0.15s for duration of100ms. The stator voltage and flux trajectory are as shown in Figure 7a) and Figure 7b) respectively. The dc link capacitor voltage rise as a result of swell is shown in Figure 7c). The stator flux trajectory follows a new circle with increased radius and settles during swell. Once the swell is removed, the flux traces back the original circle.

The PSDVR action is capable enough to restore the stator voltage during symmetrical voltage swell of DFIG. The restored stator voltage is shown in Figure8a). As the stator voltage is restored within 2 half cycles the stator flux trajectory traces the initial stable flux with a small deviation in its path due to this initial delay as shown in Figure 8b). The proposed PSDVR is successful in stabilizing the dc link capacitor voltage of DFIG and thus the rotor voltage during

HVRT as shown in Figure 8c). The results reveal promising action from PSDVR in addressing the voltage swell issue of grid connected DFIG.

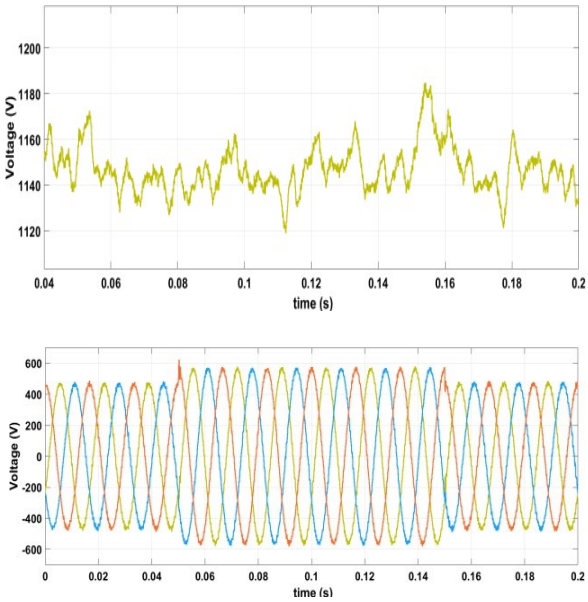

Fig. 7(a): *Stator Voltage with 1.2p.u Swell in all the Three Phases.*

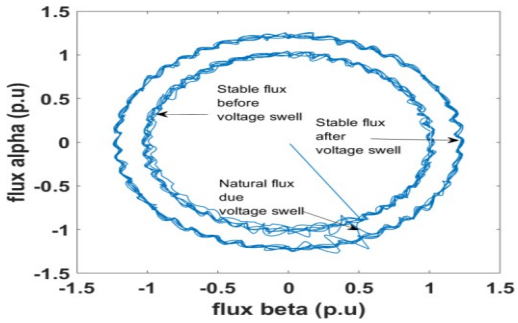

Fig. 7(b): *Stator Flux Trajectory due to Symmetrical Voltage Swell.*

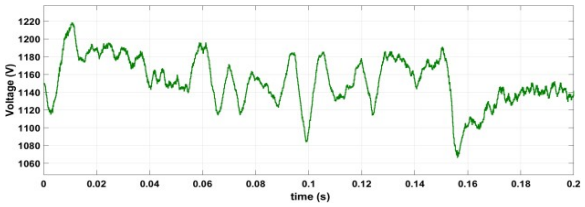

Fig. 7(b): *DC Link Capacitor with Symmetrical Voltage Swell.*

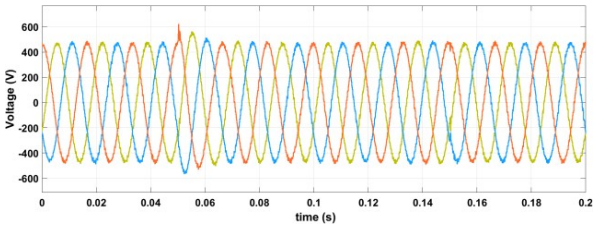

Fig. 8(a): *PSDVR Restored Stator Voltage during Symmetrical Voltage Swell.*

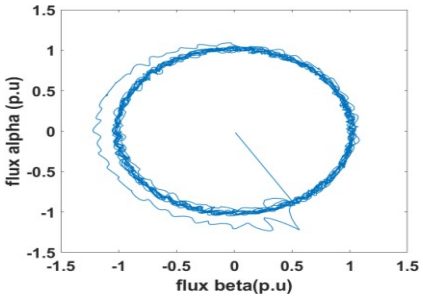

Fig. 8(b): *PSDVR Restored Stator Flux Trajectory during Symmetrical Voltage Swell.*

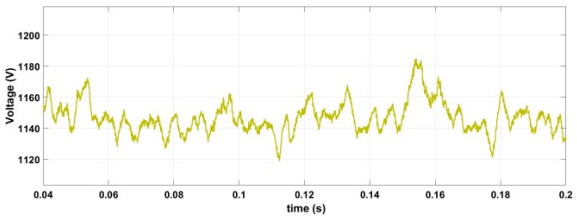

Fig. 8(c): *DC Link Capacitor Voltage after PSDVR Action.*

CONCLUSION

High voltage ride through is gradually becoming a mandatory requirement of several grid codes followed world-wide. The grid connected generators should remain connected to the grid during voltage swell as prescribed by the HVRT characteristics followed by countries. In the proposed paper dynamic voltage restorer (DVR) used for voltage sag compensation is modified in the control strategy to aid the HVRT requirement in DFIG. The proposed control strategy injects a phase shifted voltage in series with the grid to reduce the voltage swell of symmetric or asymmetric nature. The PID controllers are optimized using Particle Swarm Optimization algorithm in MATLAB using transfer functions derived

for PSDVR. The results in dicate that issues of voltage swell, flux rise and rotor voltage rise that can damage RSC of DFIG is controlled effectively with the proposed PSDVR.

Appendix

Table 1: *DFIG Generator Data.*

Rated Power	1.5MW
Rated Stator Voltage	575V
Rated stator current	1414A
DC Link capacitance voltage	1150V
Stator Resistance, Inductance	0.02 p.u,0.3p.u
Rotor Resistance, Inductance	0.016p.u,0.16p.u
Mutual Inductance	3 p.u
Pole pairs	3

Table 2: *PSDVR Data.*

Percentage Compensation, m	20%
Filter Inductance, L	9.5μH
Filter Capacitance, C	10μF
Compensation Capacity of DVR	-0.22 MW
Series Transformer MVA	0.47 MVA

REFERENCES

1. Lopez, J., Sanchis, P., Roboam, X., &Marroyo, L. (2007). Dynamic behavior of the doubly fed induction generator during three-phase voltage dips. *IEEE Transactions on Energy conversion*, 22(3), 709-717.
2. Rahimi, M., &Parniani, M. (2014). Low voltage ride-through capability improvement of DFIG-based wind turbines under unbalanced voltage dips. *International Journal of Electrical Power & Energy Systems*, 60, 82-95.
3. Ling, Y., Cai, X., & Wang, N. (2013). Rotor current transient analysis of DFIG-based wind turbines during symmetrical voltage faults. *Energy Conversion and Management*, 76, 910-917.
4. Causebrook, A., Atkinson, D. J., & Jack, A. G. (2007). Fault ride-through of large wind farms using series dynamic braking resistors (March 2007). *IEEE Transactions on power systems*, 22(3), 966-975.
5. Liang, J., Qiao, W., & Harley, R. G. (2010). Feed-forward transient current control for low-voltage ride-through enhancement of DFIG wind turbines. *IEEE Transactions on Energy Conversion*, 25(3), 836-843.
6. Peng, L., Francois, B., & Li, Y. (2009, February). Improved crowbar control strategy of DFIG based wind turbines for grid fault ride-through. In *2009 twenty-fourth annual IEEE applied power electronics conference and exposition* (pp. 1932-1938). IEEE.
7. Hossain, M. J., Pota, H. R., & Ramos, R. A. (2012). Improved low-voltage-ride-through capability of fixed-speed wind turbines using decentralised control of STATCOM with energy storage system. *IET generation, transmission & distribution*, 6(8), 719-730.
8. Wessels, C., Gebhardt, F., & Fuchs, F. W. (2010). Fault ride-through of a DFIG wind turbine using a dynamic voltage restorer during symmetrical and asymmetrical grid faults. *IEEE Transactions on Power Electronics*, 26(3), 807-815.
9. Ramirez, D., Martinez, S., Platero, C. A., Blazquez, F., & De Castro, R. M. (2010). Low-voltage ride-through capability for wind generators based on dynamic voltage restorers. *IEEE Transactions on Energy Conversion*, 26(1), 195-203.
10. Xie, Z., Zhang, X., Zhang, X., Yang, S., & Wang, L. (2014). Improved ride-through control of DFIG during grid voltage swell. *IEEE Transactions on Industrial electronics*, 62(6), 3584-3594.
11. Deng, Y., Xing, Z., & Zhang, Q. (2018). Analysis of electromagnetic transient characteristics of doubly-fed induction generator under grid voltage swell. *CPSS Transactions on Power Electronics and Applications*, 3(2), 111-118.
12. Ahmad, A., &Loganathan, R. (2010, December). Development of LVRT

and HVRT control strategy for DFIG based wind turbine system. In *2010 IEEE international energy conference* (pp. 316-321). IEEE.

13. Wang, Y. K., & Wang, J. S. (2016, May). Optimization of PID controller based on PSO-BFO algorithm. In *2016 Chinese Control and Decision Conference* (CCDC) (pp. 4633-4638). IEEE.
14. Kassarwani, N., Ohri, J., & Singh, A. (2019). Performance analysis of dynamic voltage restorer using improved PSO technique. *International Journal of Electronics*, 106(2), 212-236.